Origin of the giant magnetic moment in epitaxial Fe_3O_4 thin films

J. Orna,[1,2,3] P. A. Algarabel,[1,3] L. Morellón,[1,2,3] J. A. Pardo,[2,4] J. M. de Teresa,[1,3] R. López Antón,[5] F. Bartolomé,[1,3] L. M. García,[1,3] J. Bartolomé,[1,3] J. C. Cezar,[6] and A. Wildes[7]

[1]*Departamento de Física de la Materia Condensada, Facultad de Ciencias, Universidad de Zaragoza, Zaragoza 50009, Spain*

[2]*Instituto de Nanociencia de Aragón, Universidad de Zaragoza, Zaragoza 50009, Spain*

[3]*Instituto de Ciencia de los Materiales de Aragón, Facultad de Ciencias, Universidad de Zaragoza-CSIC, Zaragoza 50009, Spain*

[4]*Departamento de Ciencia y Tecnología de Materiales y Fluidos, Universidad de Zaragoza, Zaragoza 50018, Spain*

[5]*Departamento de Física Aplicada, Universidad de Castilla la Mancha, Ciudad Real 13071, Spain*

[6]*European Synchrotron Radiation Facility, BP 220, F-38043 Grenoble Cedex, France*

[7]*Institute Laue-Langevin, BP 156, 38042 Grenoble Cedex, France*

(Received 1 February 2010; revised manuscript received 25 March 2010; published 15 April 2010)

We study the enhanced magnetic moment observed in epitaxial magnetite (Fe_3O_4) ultrathin films ($t < 15$ nm) grown on MgO (001) substrates by means of pulsed laser deposition. The Fe_3O_4 (001) thin films exhibit high crystallinity, low roughness, and sharp interfaces with the substrate, and the existence of the Verwey transition at thicknesses down to 4 nm. The evolution of the Verwey transition temperature with film thickness shows a dependence with the antiphase boundaries density. Superconducting quantum interference device (SQUID) and vibrating sample magnetometry measurements in ultrathin films show a magnetic moment much higher than the bulk magnetite value. In order to study the origin of this anomalous magnetic moment, polarized neutron reflectivity (PNR), and x-ray magnetic circular dichroism (XMCD) experiments have been performed, indicating a decrease in the magnetization with decreasing sample thickness. X-ray photoemission spectroscopy measurements show no metallic Fe clusters present in the magnetite thin films. Through inductively coupled plasma mass spectroscopy and SQUID magnetometry measurements performed in commercial MgO (001) substrates, the presence of Fe impurities embedded within the substrates has been observed. Once the substrate contribution has been corrected, a decrease in the magnetic moment of magnetite thin films with decreasing thickness is found, in good agreement with the PNR and XMCD measurements. Our experiments suggest that the origin of the enhanced magnetic moment is not intrinsic to magnetite but due to the presence of Fe impurities in the MgO substrates.

DOI: 10.1103/PhysRevB.81.144420 PACS number(s): 75.70.Rf, 75.70.Ak, 75.50.Bb

I. INTRODUCTION

Half-metallic compounds are materials with only one spin direction at the Fermi level, which makes them desirable for their implementation in spintronic devices.[1] Magnetite (Fe_3O_4) is a half-metallic ferromagnet actively investigated due to its high Curie temperature (860 K) (Ref. 2) and its characteristic metal-insulator transition at 120 K (Verwey transition).[3–5]

Differences between some properties of bulk magnetite and epitaxial thin films have been observed, such as an increased resistivity with decreasing film thickness,[6–8] negative magnetoresistance,[9–11] decreased and broadened Verwey transition temperature (T_V),[7,12,13] superparamagnetism in ultrathin films,[14,15] decreased saturation magnetization,[16–19] and anomalous, planar, and ordinary Hall effects.[20–22] This anomalous behavior has often been associated to the film microstructure and the presence of structural growth defects called antiphase boundaries (APBs).[17,18]

There are two forms of symmetry breaking in $Fe_3O_4 \| MgO$ (001) epitaxy, leading to the creation of structural defects during the growth process known as antiphase boundaries. The first one is due to the fact that Fe_3O_4 has twice the unit-cell size of MgO. This implies that neighboring islands may not coalesce with matching cation sublattices when the film nucleates and grows on the surface of the substrate, leading to a boundary formation during the growth process. The other one is due to the fact that the Fe_3O_4 ($Fd3m$) crystal structure is lower in symmetry than that of MgO ($Fm3m$). Therefore, the MgO unit cell can be rotated by 90° around an axis perpendicular to the interface, whereas Fe_3O_4 cannot, also resulting in the formation of APBs.

Across the APBs the oxygen lattice remains undisturbed while the cation lattice is displaced, therefore, the system remains monocrystalline. Although it was first believed that the APBs formed at the very first stages of the growth and that the domain size was constant,[15] Eerenstein *et al.*[8,23] demonstrated that the APBs domain size (D) increases significantly with deposition time and therefore, the antiphase domains are largest in the thickest magnetite films due to the prolonged deposition time, following:

$$D \propto \sqrt{t}, \tag{1}$$

where t is the film thickness. Therefore, the APB density decreases significantly with the increase in film thickness (t).[6]

Finally, APBs have been observed in Fe_3O_4 films grown on $MgAl_2O_4$ and related to the absence of epitaxial strain relaxation,[24] as if the APBs network leads to the formation of areas with opposite sign of stress, compensating and reducing the effective stress experienced by the films. Thus, APBs can be considered as a strain relaxation mechanism.[24,25]

In bulk magnetite the dominating magnetic coupling is the antiferromagnetic superexchange between neighboring tetrahedral and octahedral cation sites, the coupling between octahedral site cations being effectively ferromagnetic. However, in Fe_3O_4 thin films, these magnetic interactions are altered at the antiphase boundaries,[15,17] across which the intrasublattice exchange interactions dominate, reversing the spin coupling. Therefore, the structural boundary separates oppositely magnetized regions and the resultant coupling between two domains turns out to be either frustrated or antiferromagnetic. These antiferromagnetic exchange interactions occurring across the APBs have been identified to be responsible for the impossibility to saturate the film magnetization in moderate magnetic fields.[17–19] The measured magnetization is, therefore, necessarily lower than the bulk one, due to this decrease in the magnetization at the APBs.

However, recent studies performed by Arora *et al.*[26,27] on well-characterized epitaxial Fe_3O_4 thin films grown on MgO (001) show that the ultrathin films (<5 nm thickness) are ferromagnetic and their magnetization is much greater than that of bulk magnetite. The main factor contributing to the observed enhanced magnetic moment is proposed to be the noncompensation of spin moments between the tetrahedral and octahedral sublattices at the surface, at the interface with the substrate, and at the antiphase-domain boundaries. They suggest a model in which the magnetite films consist of a layer with bulk properties (bulk saturation magnetization M_S) plus surface contribution of moment M_i at the Fe_3O_4-MgO and Fe_3O_4-air interfaces, resulting in a magnetization given by

$$M = M_S + \frac{M_i}{t}, \tag{2}$$

where t is the film thickness.

Similar results have been found for the spinel ferrite $NiFe_2O_4$ grown on $SrTiO_3$ substrates,[28] showing for 3-nm-thick films a magnetization enhancement of almost four times the bulk value, as measured by means of SQUID magnetometry. This effect was ascribed to the cation inversion: the presence of Ni^{2+} in A sites and Fe^{3+} in B sites would increase the magnetic moment. However, recent x-ray magnetic circular dichroism (XMCD) and resonant photoemission experiments have ruled out this hypothesis.[29]

We have obtained similar magnetization results to those reported by Arora,[26,27] therefore, the purpose of the present work is to investigate further the origin of the anomalous giant magnetic moment in epitaxial Fe_3O_4 thin films grown on MgO (001). In Sec. II we summarize the preparation and characterization of the thin films. The magnetic behavior is studied in Sec. III with four complementary techniques: superconducting quantum interference device (SQUID) and vibrating sample magnetometry (VSM), polarized neutron reflectivity (PNR), and XMCD, showing conflicting results obtained for the magnetization behavior as a function of film thickness. The chemical analysis of the films by x-ray photoemission spectroscopy (XPS) has also been investigated. Finally, the origin of the enhanced magnetic moment is proposed to stem from the Fe impurities found in the MgO substrates by means of inductively coupled plasma (ICP) mass spectroscopy and SQUID measurements. Conclusions are summarized in Sec. IV.

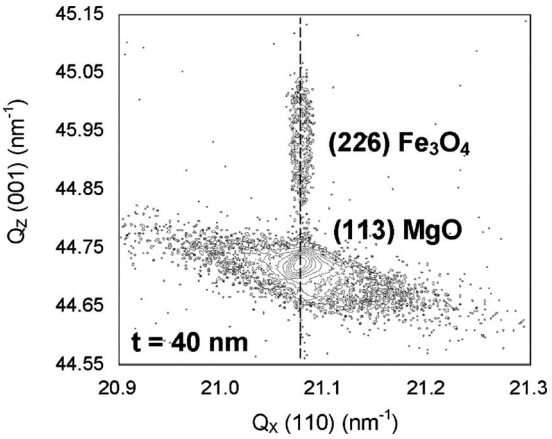

FIG. 1. Reciprocal space map in the vicinity of the asymmetrical 113 MgO and 226 Fe_3O_4 reflections. Q_x and Q_z are along the reciprocal space (110) and (001) directions, respectively.

II. EXPERIMENTAL

Fe_3O_4 films of thicknesses ranging from 3 to 350 nm were deposited on MgO (001) substrates by pulsed laser deposition (PLD) using a KrF excimer laser with 248 nm wavelength, 10 Hz repetition rate, and 3×10^9 W/cm^2 irradiance in an ultrahigh-vacuum chamber. The film thicknesses were measured by x-ray reflectivity (XRR). Further details on the growth and characterization can be found elsewhere.[31]

The stoichiometric Fe_3O_4 target was prepared from Fe powder (99.9% purity) by solid-state reaction. X-ray diffraction, magnetic, and transport measurements of the target indicate the desired Fe_3O_4 stoichiometry and physical properties.[30] The final target density is close to the theoretical value, which is suitable for appropriate laser ablation.

The base pressure in the deposition chamber was lower than 10^{-8} Torr. The substrate was kept in vacuum at a temperature of 450 °C during laser ablation of the target. Single crystal MgO (001) (cubic lattice parameter a_s=4.21 Å) from CRYSTAL GmbH, was chosen as a substrate because of the small lattice mismatch with bulk Fe_3O_4 (cubic lattice parameter a=8.40 Å).

The presence of the 004 reflection from the Fe_3O_4 film near the 002 Bragg peak from the MgO substrate in a symmetrical $\theta/2\theta$ x-ray scan (not shown here) confirms the expected out-of-plane orientation $Fe_3O_4[001]\|MgO[001]$. The observed Laue oscillations up to tenth order in the 40-nm-thick films are an indication of a very high crystalline coherence.[31] The presence of the asymmetrical 226 reflection from a 40-nm-thick magnetite film in the reciprocal space map performed near the asymmetrical 113 MgO reflection (Fig. 1) demonstrates the in-plane orientation $Fe_3O_4[110]\|MgO[110]$, and the match of the Fe_3O_4 and MgO in-plane lattice parameter indicates the absence of epitaxial strain relaxation in the 40-nm-thick film.

High-resolution transmission electron microscopy cross-sectional images obtained from 40-nm-thick films (not

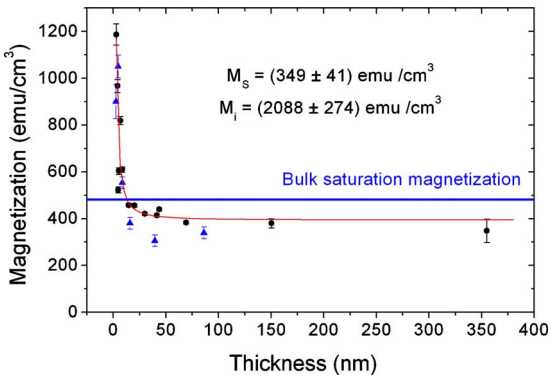

FIG. 2. (Color online) Saturation magnetization measured at 300 K as a function of the film thickness at 5 T for the standard magnetite films (black dots) and at 1.9 T for samples grown specifically for PNR measurements (blue triangles). The solid line represents a fit to the data using Eq. (2), $M=M_S+M_i/t$, where M_S and M_i are the bulk saturation magnetization and the surface contribution, respectively, and t the thickness of the film.

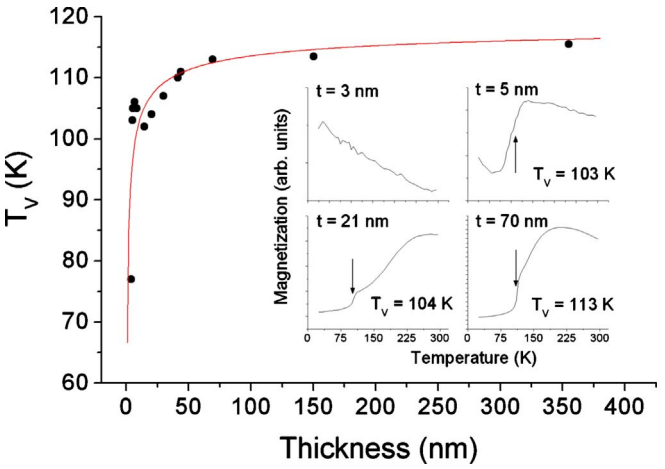

FIG. 3. (Color online) Verwey transition temperature as a function of Fe_3O_4 films thickness measured in an applied magnetic field of 500 Oe. The samples were previously zero field cooled down to 5 K. The inset shows the magnetization signal as a function of temperature for various film thicknesses.

shown here) evidence that the films are homogeneous and continuous at lateral sizes of the order of microns, and that the interface between the Fe_3O_4 and the MgO substrate is steep at the atomic level.[32] Electron diffraction experiments, also published elsewhere indicate the expected cubic structure of (a) MgO and (b) Fe_3O_4, with additional diffraction spots at intermediate positions with respect to the MgO image due to the doubling of the lattice parameter in Fe_3O_4.[32]

Magnetization measurements have been performed in commercial SQUID and VSM magnetometers. The SQUID is an MPMS-XL model from Quantum Design Ltd. with RSO option (reciprocating sample option). The substrate size for magnetization measurements was $5\times5\times0.5$ mm^3, the measurement scan length was 4 cm, and no size correction was applied. The VSM is from ADE Technologies (now MicroSense) model EV7 and operates at 75 Hz.

PNR measurements were performed at the Institut Laue-Langevin on the D17 vertical sample plane reflectometer with an applied in-plane magnetic field of 1 T at room temperature. Since the applied field was large enough to mostly saturate the sample, all of the magnetization is essentially parallel to the applied field, thus, the spin-flip scattering is negligible.

X-ray absorption (XAS) and XMCD experiments at the $L_{2,3}$ Fe absorption edges were performed at the ID08 beamline of the ESRF in Grenoble. The XMCD experiments were carried out at 300 K under an applied field of ±2.5 T, with total electron yield detection and a $\sim$100% polarization rate.

The XPS analysis was performed with an Axis Ultra DLD (Kratos Tech.) spectrometer with a monochromatized Al K_α source (1486.6 eV) run at 15 kV and 10 mA under a residual pressure of 10^{-7} Pa. The binding energies (BEs) were referenced to the C 1s peak from carbon at 284.9 eV.

III. RESULTS AND DISCUSSION

The magnetic hysteresis loops were measured at room temperature up to 5 T using a SQUID by applying the magnetic field in the film plane along the [100] direction. Figure 2 shows the dependence of the magnetization with the film thickness, ranging from 2.8 to 300 nm. The saturation magnetization values have been determined by fitting the high-field data to a linear dependence in order to subtract the slope of the hysteresis loops due to the MgO substrate contribution.

For the films with thickness greater than 20 nm, the obtained magnetization values are about 10–15 % less than the value reported for bulk Fe_3O_4 (480 emu/cm^3 or 4 μ_B/f.u.), which is in agreement with results published previously by other authors.[17–19]

The magnetite films with thicknesses below 20 nm exhibit increasing magnetization values as the thicknesses are reduced, up to values significantly larger than the bulk magnetic moment. The saturation magnetization values shown in Fig. 2 have been fitted to the expression in Eq. (2), as suggested by Arora *et al.*,[26,27] obtaining a bulk saturation magnetization $M_S=349\pm41$ emu/cm^3 and a surface contribution $M_i=2088\pm274$ emu/cm^3, in agreement with.[26,27]

The presence of the Verwey transition down to 4-nm-thick films (Fig. 3) evidences the high quality of the films. A decrease in T_V for decreasing Fe_3O_4 thicknesses is observed, which has been previously reported by other authors,[7,19,33] and explained as a slight nonstoichiometry of the films[33,34] or strain due to the epitaxial growth on the substrate.[7] Recently, it has been suggested[8,19] that in ultrathin films where the APBs domain size is small, the long-range order of the Fe^{2+} and Fe^{3+} ions at the octahedral sites, necessary for the Verwey transition to occur, can be inhibited,[35] producing a decrease in T_V. Indeed, this decrease in the Verwey transition temperature as a function of Fe_3O_4 film thickness (t) can be fitted to the phenomenological expression given by Eq. (3), obtaining an exponent $n=-0.4\pm0.1$, and $b=0.4\pm0.1$,

$$T_V = T_V^{Bulk}(1-bt^n). \tag{3}$$

As the APBs domain size (D) depends on the thickness of the magnetite films according to the relation given in Eq. (1),

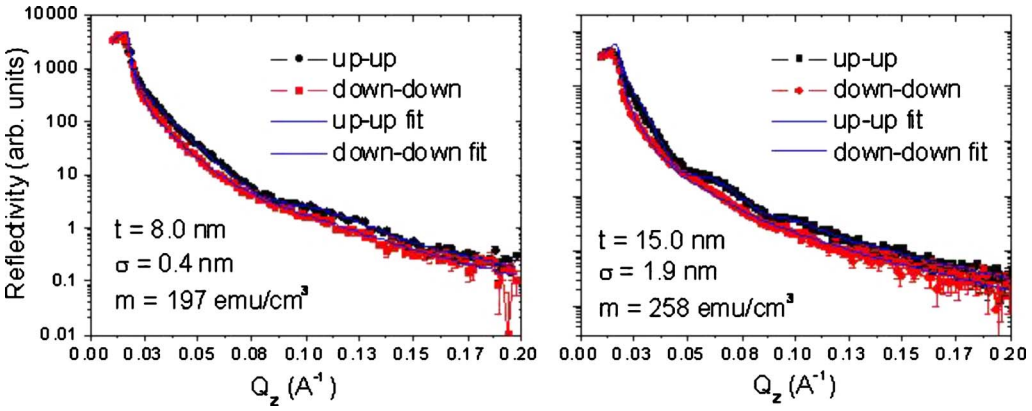

FIG. 4. (Color online) PNR measurements of 15- and 8-nm-thick Fe_3O_4 (001) thin films in a 1 T in-plane field at $T=300$ K. The dotted and squared curves correspond, respectively, to the reflection of up and down polarized neutrons, whereas the solid lines correspond to the fit.

it can be deduced that T_V decreases with decreasing domain size, and thus with increasing APBs density, as expected.

PNR measurements have been performed in order to understand the anomalous magnetic behavior of the magnetite ultrathin films, as the PNR is a specially suited technique to the measurement of magnetization and magnetic depth profile in thin films. Therefore, it may determine whether the enhanced magnetic moment is confined at the surface of the film, at the interface with the substrate, or is homogeneously distributed over the film thickness. Figure 4 displays the PNR measurements together with numerical fits represented by solid lines as calculated by means of GENX software,[36] with film thickness, roughness, and magnetic moment, and substrate roughness used as variable parameters. Thickness (t) and surface roughness (σ) parameters are consistent with previously performed XRR measurements (not shown here; $t \pm \sigma = 8.6 \pm 0.5$ nm and 15.8 ± 0.4 nm). Atomic force microscopy (not shown here) yields root-mean-square roughness in the range 0.1–0.5 nm, i.e., same value as in the as-received MgO substrates. Moreover, the experimental data are well reproduced when the model used for the fit corresponds to a single layer with a homogeneous magnetic moment throughout the film. However, this is in contrast to the magnetic contribution from the film surface or from the interface of the film with the substrate suggested in Ref. 27. Indeed, the magnetic moment m obtained from the fit is always lower than the bulk value of 480 emu/cm^3. While the 8-nm-thick film, has a magnetization value of 553 emu/cm^3 (115% of the bulk value) obtained from the VSM magnetometry measurement, the PNR data reveal a magnetization of 197 emu/cm^3 (41% of the bulk value). Regarding the 15-nm-thick film, its saturation magnetization is lower than the bulk value in both sets of measurements but it is even lower in the case of PNR:380 emu/cm^3 from VSM and 258 emu/cm^3 from PNR. Previous PNR studies in Fe_3O_4/NiO and Fe_3O_4/CoO exchange biased multilayers, where the thickness of the Fe_3O_4 layers are 15–16 nm, yield a magnetic moment close to that of bulk in the center of the Fe_3O_4 layers and a noticeable reduction toward the interfaces.[37] It is evident that the enhanced magnetic signal from the SQUID or VSM measurements cannot be due to any surface or interface magnetic contribution from the film.

To investigate the origin of the magnetic moment observed in the films we have also performed XAS and XMCD in 8 nm and 58 nm Fe_3O_4 films. The data are shown in Fig. 5. XAS curves (top panel) are plotted as obtained from the average of the left and right circularly polarized light absorption, together with a bulk magnetite sample for comparison. Once normalized to the absorption edge jump obtained well above the edges ($E_N \sim 750$ eV) in a bulk single-crystal sample,[38] the white lines for the films are slightly higher than that obtained for the bulk, indicating that the number of 3d holes in the Fe 3d band is somehow enhanced. This effect may be related with surface effects or APBs. The shape of the XAS curves of the films evidences the absence of any substantial amount of metallic iron in the films. Figure 5 (lower panel) shows the XMCD curves of both samples, which are in good agreement with the corresponding spectra of Fe_3O_4 thin films[39] and of a variety of sizes of iron oxide

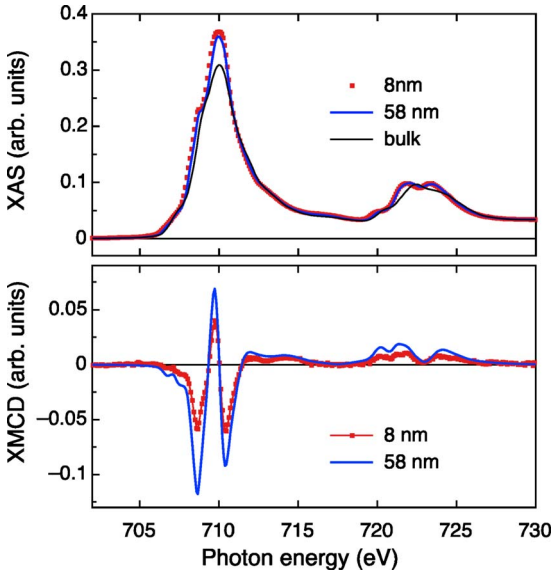

FIG. 5. (Color online) Top panel: XAS curves obtained from the average of the left and right circularly polarized light absorption, for two of the samples and bulk magnetite (as reference). Down panel: XMCD experiment performed at 300 K under an applied magnetic field of ± 2.5 T for the same samples.

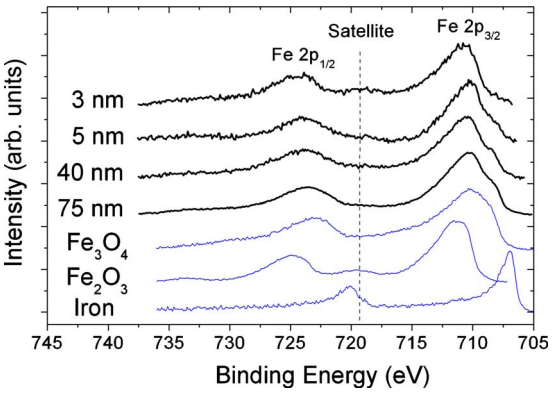

FIG. 6. (Color online) XPS measurements on the Fe $2p$ core-level spectrum in magnetite thin films with thicknesses 3, 5, 40, and 75 nm. The data are plotted together with XPS spectra of pure α-Fe_2O_3, Fe_3O_4, and Fe.

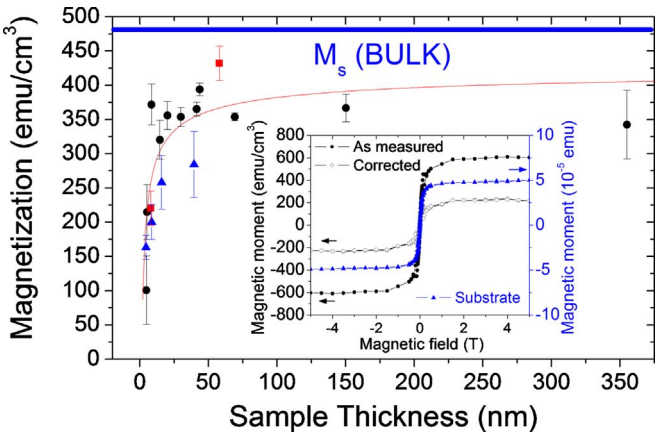

FIG. 7. (Color online) Magnetization measured at 300 K as a function of the film thickness after the magnetic signal from the MgO (001) substrates was corrected. The solid line represents a fit to the data using Eq. (4). Block squares (red) are used for the XMCD data, block triangles (blue) are used for the PNR fits, and block circles (black) are used for the corrected SQUID data. The inset displays the SQUID measurements for a representative 4.5 nm sample as measured (emu/cm^3, block black circles) and corrected after subtracting the signal from the substrate (emu/cm^3, open black circles). The total magnetic moment from the substrate is also displayed (emu, block blue triangles).

nanoparticles.[40] The sum-rule analysis of the XMCD curves allows obtaining the Fe magnetic moments in the oxide films.[41,42] The number of Fe $3d$ holes used for the analysis (14.1 and 14 holes in the $3d$ band per formula unit for the 8 and the 58 nm films, respectively) has been estimated from the integral of the XAS white lines taking as reference the bulk value (13.5 holes/f.u.). The magnetization obtained at 2.5 T in these two samples is 432 emu/cm^3 (or 3.6 μ_B/f.u.) for the 58 nm film and 220 emu/cm^3 for the 8 nm film (corresponding to 1.83 μ_B/f.u.), both in very good agreement with the PNR values. Given the mean-free path of a ~710 eV photon in magnetite (~150 nm) and MgO (~500 nm), our result shows that the magnetic moment observed by PNR is entirely due to Fe_3O_4, as the technique probes the average magnetization of the whole film while only 1 in 2000 Fe impurities (for a 1-mm-thick substrate) are excited by the x-ray beam before its total attenuation. Although a precise determination of the orbital to spin ratio in magnetite requires to extend the XMCD experiment in a much wider energy range,[43] we estimate that $\mu_L/\mu_S < 0.05$ in our samples.

In order to discern the existence of Fe clusters in the film, whose presence could lead to an enhanced magnetization that cannot be properly measured with PNR or XMCD, XPS measurements were performed on the Fe $2p$ core-level spectrum in selected magnetite thin films. The iron and its various oxides (α-Fe_2O_3, Fe_3O_4, and FeO among others) can be distinguished from each other by their characteristic satellite peaks. Figure 6 shows the XPS spectra of 3-, 5-, 40-, and 75-nm-thick magnetite films, and the spectra from pure bulk Fe_3O_4, Fe_2O_3, and Fe powder samples. The BE peak at 706.6 eV, characteristic of metallic Fe $2p_{3/2}$ cannot be observed in any of our films, leading to the conclusion that there are no metallic Fe clusters and, thus, the origin of the enhanced magnetic moment is definitely not intrinsic to the magnetite film. The Fe $2p_{3/2}$ satellite binding energy is different for the Fe^{2+} or Fe^{3+} valence states: BE=715.5 eV in FeO and BE =719 eV, in α-Fe_2O_3, in the case of Fe_3O_4 both satellites are present, which produces an unresolved peak. However, it is possible to observe that in the case of the thinner films (3 nm thick), the $2p_{3/2}$ satellite increases its intensity and its position can be distinguished near BE=719 eV, indicating a deviation of the stoichiometry toward an α-Fe_2O_3 enriched phase which should lead to a decrease in the saturation magnetization, in opposition to the magnetic measurements performed through SQUID and VSM.

The possible sources of experimental error in the observation of nanoscale magnetism have been recently reported.[44] When measuring small signals (below 10^{-4} emu), magnetic traces are introduced in our samples when handling them or due to impurities in the sample substrates, so they must be considered in the analysis. Therefore, as the enhanced magnetic moment was only found in the case of SQUID and VSM measurements, and PNR and XMCD are insensitive to the substrate, a study of the MgO substrates is strongly required.

ICP mass spectrometry measurements of the MgO (001) substrates, provided by our substrate commercial provider Crystal GbmH, showed the existence of Fe impurities with a concentration $\leq$5 ppm (other impurities found are: Ca 12.6, Al 3.8, Si 4.9 Cr 0.3, and B 0.6, all values in parts per million). This concentration is enough to provide a magnetic signal of approximately 50 μemu in each ($5\times5\times0.5$) mm^3 substrate. SQUID with RSO measurements were performed in a MgO (001) substrate in order to confirm the Fe impurities presence and a typical ferromagnetic loop was obtained with a saturation magnetization of 11 μemu measured at a maximum magnetic field of 5 T, which corresponds to a concentration of 1 ppm Fe impurities.

We have corrected the saturation magnetization data by subtracting the substrate magnetic signal assuming a maximum Fe contribution of approximately 50 μemu (Fig. 7, inset). The resulting values show a decrease in the magnetization when decreasing magnetite film thicknesses (Fig. 7),

as reported previously in the literature.[17–19] The magnetization of our Fe_3O_4 films can be modeled as a layer with M_S which decreases as the film thickness decreases. The corrected magnetization data follow the same phenomenological law as that obtained for the Verwey Temperature,

$$M = M_S(1 - b't^n). \tag{4}$$

If M_S and b' are taken as free parameters, the optimal fit is found when $n=-0.5$ and we obtain: $M_S = 430.7 \pm 35.2$ emu/cm^3 and $b' = 1.1 \pm 0.2$. The value obtained from the fit $M_S = 431$ emu/cm^3 is lower (10%) than the saturation magnetization reported for bulk magnetite (480 emu/cm^3). This can be explained as a nonsaturation of the samples in the magnetic field where the saturation magnetizations were measured (5 T) due to the presence of APBs.[17–19]

As the APBs domain size (D) depends on the thickness of the magnetite films according to the relation given by Eq. (1), the magnetization depends on D,

$$M = M_S\left(1 - \frac{c}{D}\right). \tag{5}$$

Therefore, it can be understood that the magnetization of the films decreases with decreasing domain size and thus with increasing APBs density.

The dependence of M_S with film thickness obtained after the substrate correction is in good agreement with the results obtained from PNR and XMCD experiments (see Fig. 7), supporting our assumption that the enhanced magnetic moment suggested by the magnetization measurements is indeed due to Fe impurities present in the MgO substrates. It is important to stress that the Fe impurities are present in the as-received substrates and not implanted during the PLD deposition of Fe_3O_4. It is known that the kinetic energy of the impinging species in PLD typically lie in the 1–100 eV range.[45,46] Nevertheless, at the low fluence used, and given the high crystallinity, low roughness, and sharp interfaces of our films, we can estimate the energy of the species arriving at the substrate being <5 eV or lower. In this range of energy, implantation in the MgO is negligible.[47] Studies of Fe implantation in MgO typically require energies in the range of 50–100 keV or higher.[48] Another interesting possibility is the existence of d^0 ferromagnetism in MgO as suggested recently in both nanoparticles[49,50] and thin films.[51] We have not found any evidence of Mg vacancies in our single crystalline substrates and, therefore, this effect may be ruled out.

IV. CONCLUSION

We have grown high-quality epitaxial $Fe_3O_4(001)$ films on MgO substrates by means of pulsed laser deposition and studied the magnetic properties, focusing on results of magnetization in ultrathin films ($t<15$ nm). Contradictory results have been obtained when comparing SQUID and VSM magnetometry with PNR and XCMD measurements. XPS experiments show absence of metallic Fe impurities in the magnetite films, whose presence could justify the enhanced magnetic moment found through SQUID and VSM measurements.

Finally, ICP and SQUID magnetometry measurements performed in standard MgO (001) substrates show the presence of Fe impurities in the substrates. The corrected thin-film magnetization as well as the Verwey transition temperature show a decrease with decreasing film thickness as α $t^{-1/2}$, which can be related to APBs density. This result together with the PNR and XMCD experiments indicate that the origin of the enhanced magnetic moment is extrinsic, due to the presence of Fe impurities in the MgO substrates, and not intrinsic to Fe_3O_4.

ACKNOWLEDGMENTS

We acknowledge fruitful discussions with A. Fernández-Pacheco about XPS measurements and with T. Charlton from ISIS about PNR. This work has been financially supported by Spanish Ministry of Science through Projects No. MAT2008-06567-C02 and No. MAT2008-01077, and the Regional Government of Aragón (E-26, E-69, and E-34).

[1] G. Prinz, J. Magn. Magn. Mater. **200**, 57 (1999).
[2] S. F. Alvarado, W. Eib, F. Meier, D. T. Pierce, K. Sattler, and H. C. Siegmann, Phys. Rev. Lett. **34**, 319 (1975).
[3] J. E. W. Verwey, Nature (London) **144**, 327 (1939).
[4] F. Walz, J. Phys.: Condens. Matter **14**, R285 (2002).
[5] J. García and G. Subías, J. Phys.: Condens. Matter **16**, R145 (2004).
[6] A. V. Ramos, J. B. Moussy, M. J. Guittet, A. M. Bataille, M. Gautier-Soyer, M. Viret, C. Gatel, P. Bayle-Guillemaud, and E. Snoeck, J. Appl. Phys. **100**, 103902 (2006).
[7] X. W. Li, A. Gupta, G. Xiao, and G. Q. Gong, J. Appl. Phys. **83**, 7049 (1998).
[8] W. Eerenstein, T. T. M. Palstra, T. Hibma, and S. Celotto, Phys. Rev. B **66**, 201101 (2002).
[9] W. Eerenstein, T. T. M. Palstra, S. S. Saxena, and T. Hibma, Phys. Rev. Lett. **88**, 247204 (2002).
[10] M. Ziese and H. J. Blythe, J. Phys.: Condens. Matter **12**, 13 (2000).
[11] T. Kado, J. Appl. Phys. **103**, 043902 (2008).
[12] S. P. Sena, R. A. Lindley, H. J. Blythe, C. Sauer, M. Al-Kafarji, and G. A. Gehring, J. Magn. Magn. Mater. **176**, 111 (1997).
[13] G. Q. Gong, A. Gupta, G. Xiao, W. Qian, and V. P. Dravid, Phys. Rev. B **56**, 5096 (1997).
[14] W. Eerenstein, T. Hibma, and S. Celotto, Phys. Rev. B **70**, 184404 (2004).
[15] F. C. Voogt, T. T. M. Palstra, L. Niesen, O. C. Rogojanu, M. A. James, and T. Hibma, Phys. Rev. B **57**, R8107 (1998).
[16] P. A. A. van der Heijden, P. J. H. Bloemen, J. M. Gaines, J. T. W. M. van Eemeren, R. M. Wolf, P. J. van der Zaag, and W. J. M. de Jonge, J. Magn. Magn. Mater. **159**, L293 (1996).
[17] D. T. Margulies, F. T. Parker, M. L. Rudee, F. E. Spada, J. N. Chapman, P. R. Aitchison, and A. E. Berkowitz, Phys. Rev. Lett.

79, 5162 (1997).
[18] D. T. Margulies, F. T. Parker, F. E. Spada, R. S. Goldman, J. Li, R. Sinclair, and A. E. Berkowitz, Phys. Rev. B **53**, 9175 (1996).
[19] J. B. Moussy, S. Gota, A. Bataille, M.-J. Guittet, M. Gautier-Soyer, F. Delille, B. Dieny, F. Ott, T. D. Doan, P. Warin, P. Bayle-Guillemaud, C. Gatel, and E. Snoeck, Phys. Rev. B **70**, 174448 (2004).
[20] A. Fernández-Pacheco, J. M. De Teresa, J. Orna, L. Morellón, P. A. Algarabel, J. A. Pardo, and M. R. Ibarra, Phys. Rev. B **77**, 100403(R), (2008).
[21] A. Fernández-Pacheco, J. M. De Teresa, J. Orna, L. Morellón, P. A. Algarabel, J. A. Pardo, M. R. Ibarra, C. Magen, and E. Snoeck, Phys. Rev. B **78**, 212402 (2008).
[22] A. Fernández-Pacheco, J. Orna, J. M. De Teresa, P. A. Algarabel, L. Morellón, J. A. Pardo, and M. R. Ibarra, Appl. Phys. Lett. **95**, 262108 (2009).
[23] W. Eerenstein, T. T. M. Palstra, T. Hibma, and S. Celotto, Phys. Rev. B **68**, 014428 (2003).
[24] M. Luysberg, R. G. S. Sofin, S. K. Arora, and I. V. Shvets, Phys. Rev. B **80**, 024111 (2009).
[25] S. K. Arora, R. G. S. Sofin, I. V. Shvets, and M. Luysberg, J. Appl. Phys. **100**, 073908 (2006).
[26] S. K. Arora, H.-C. Wu, H. Yao, W. Y. Ching, R. J. Choudhary, I. V. Shvets, and O. N. Mryasov, IEEE Trans. Magn. **44**, 2628 (2008).
[27] S. K. Arora, H.-C. Wu, R. J. Choudhary, I. V. Shvets, O. N. Mryasov, H. Yao, and W. Y. Ching, Phys. Rev. B **77**, 134443 (2008).
[28] U. Lüders, M. Bibes, J. F. Bobo, M. Cantoni, R. Bertacco, and J. Fontcuberta, Phys. Rev. B **71**, 134419 (2005).
[29] M. C. Richter, J. M. Mariot, O. Heckmann, L. Kjeldgaard, B. S. Mun, C. S. Fadley, U. Lüders, J. F. Bobo, P. de Padova, A. Taleb-Ibrahimi, and K. Hricovini, Eur. Phys. J. Spec. Top. **169**, 175 (2009).
[30] D. Serrate, J. M. De Teresa, P. A. Algarabel, R. Fernández-Pacheco, M. R. Ibarra, and J. Galibert, J. Appl. Phys. **97**, 084317 (2005).
[31] J. M. De Teresa, A. Fernández-Pacheco, L. Morellón, J. Orna, J. A. Pardo, D. Serrate, P. A. Algarabel, and M. R. Ibarra, Microelectron. Eng. **84**, 1660 (2007).
[32] J. Orna, L. Morellon, P. A. Algarabel, J. A. Pardo, S. Sangiao, C. Magen, E. Snoeck, J. M. De Teresa, and M. R. Ibarra, IEEE Trans. Magn. **44**, 2862 (2008).
[33] E. Lochner, K. A. Shaw, R. C. DiBari, W. Portine, P. Stoyonov, S. D. Berry, and D. M. Lind, IEEE Trans. Magn. **30**, 4912 (1994).
[34] P. J. van der Zaag, W. F. J. Fontjin, P. Gaspard, R. M. Wolf, V. A. M. Brabers, R. J. M. van der Veerdonk, and P. A. A. Van der Heijden, J. Appl. Phys. **79**, 5936 (1996).
[35] J. P. Wright, J. P. Attfield, and P. G. Radaelli, Phys. Rev. Lett. **87**, 266401 (2001).
[36] M. Björck and G. Andersson, J. Appl. Crystallogr. **40**, 1174 (2007).
[37] A. R. Ball, A. J. G. Leenaers, P. J. van der Zaag, K. A. Shaw, B. Singer, D. M. Lind, H. Frederikze, and M. Th. Rekveldt, Appl. Phys. Lett. **69**, 1489 (1996); A. R. Ball, H. Frederikze, D. M. Lind, R. M. Wolf, P. J. H. Bloemen, M. Th. Rekveldt, and P. J. van der Zaag, Physica B **221**, 388 (1996).
[38] T. Saitoh, A. E. Bocquet, T. Mizokawa, and A. Fujimori, Phys. Rev. B **52**, 7934 (1995).
[39] P. Kuiper, B. Searle, L.-C. Duda, R. M. Wolf, and P. J. van der Zaag, J. Electron Spectrosc. Relat. Phenom. **86**, 107 (1997).
[40] J. Park, K. An, Y. Hwang, J.-G. Park, H.-J. Noh, J.-Y. Kim, J.-H. Park, N.-M. Hwang, and T. Hyeon, Nature Mater. **3**, 891 (2004).
[41] B. T. Thole, P. Carra, F. Sette, and G. van der Laan, Phys. Rev. Lett. **68**, 1943 (1992).
[42] P. Carra, B. T. Thole, M. Altarelli, and X. Wang, Phys. Rev. Lett. **70**, 694 (1993).
[43] N. Pérez, F. Bartolomé, L. M. García, J. Bartolomé, M. P. Morales, C. J. Serna, A. Labarta, and X. Batlle, Appl. Phys. Lett. **94**, 093108 (2009).
[44] M. A. Garcia, E. Fernandez Pinel, J. De la Venta, A. Quesada, V. Bouzas, J. F. Fernández, J. J. Romero, M. S. Martín González, and J. L. Costa-Krämer, J. Appl. Phys. **105**, 013925 (2009).
[45] *Pulsed Laser Deposition of Thin Films*, edited by D. B. Chrisey and G. K. Hubler (Wiley Interscience, New York, 1994).
[46] P. R. Willmott, Prog. Surf. Sci. **76**, 163 (2004).
[47] J. F. Ziegler, J. P. Biersack, and U. Littmark, *The Stopping and Range of Ions in Solids* (Pergamon, New York, 1985); SRIM code: http://www.srim.org
[48] N. Hayashi, I. Sakamoto, T. Toriyama, H. Wakabayashi, T. Okada, and K. Kuriyama, Surf. Coat. Technol. **169-170**, 540 (2003); Z. Mao, Z. He, D. Chen, W. Y. Cheung, and S. P. Wong, Solid State Commun. **142**, 329 (2007).
[49] J. F. Hu, Z. I. Zhang, M. Zhao, H. W. Qin, and M. H. Jiang, Appl. Phys. Lett. **93**, 192503 (2008).
[50] J. I. Beltran, C. Monty, Ll. Balcells, and C. Martinez-Boubeta, Solid State Commun. **149**, 1654 (2009).
[51] C. Martinez-Boubeta, J. I. Beltran, Ll. Balcells, Z. Konstantinovic, S. Valencia, D. Schmitz, J. Cornil, and B. Martínez (unpublished).